

# A review of full-scale wind-field measurements of the wind-turbine wake effect and a measurement of the wake-interaction effect

Haiying Sun<sup>a</sup>, Xiaoxia Gao<sup>b</sup>, Hongxing Yang<sup>a\*</sup>

<sup>a</sup>Renewable Energy Research Group, Department of Building Services Engineering, The Hong Kong Polytechnic University, Hong Kong

<sup>b</sup>Department of Power Engineering, North China Electric Power University (Baoding), Baoding, PR China

## Abstract

This paper provides an overview of full-scale wind field measurements of the wind-turbine wake effect and presents the results and experience of performing a new measurement. First, typical onshore wind-farm measurements are reviewed and summarized, followed by a description of the measurements used in offshore wind farms. Then, the measurements obtained for studying isolated wake effects are introduced. Information about the location, equipment, and process used in a number of experiments are described in detail, followed by a discussion of significant results, an economic analysis, and the experimental difficulties encountered. Validation of a wake model has been the main purpose of some studies, which are also reviewed in this paper. Lastly, the results of a new experiment on the wake interaction effect are presented and summarized. The work presented in this paper advances our understanding of the development process and research status of full-scale wind field measurements of the wake effect. Suggestions are also made regarding future measurements.

Keywords: Wake effect; Wind field measurements; Experimental procedures; Measurement of wake interaction.

## 1. Introduction

Wind energy, widely accepted as a clean and renewable energy source, is playing an important role in many regions of the world [1]. As the number of wind turbines erected in wind farms increases, the influence of the wake effect and wake-generated loads tend to become more significant [2]. The wake of a wind turbine (WT) occurs in the downstream volume, which is affected by the WT absorbing momentum from the inflow, resulting in a reduction of the downwind speed. However, the flow in the wake is more turbulent than that in the inflow. This is due to the fact that the rotation of the WT blades generates turbulence and that the WT itself is an obstacle to the inflow [3]. In wind farms, downwind WTs suffer from structural loads and wind-speed deficits caused by the wakes of upstream WTs. This degradation in performance has an important effect on the benefits obtained by wind farms. Therefore, a better understanding of wake characteristics is essential to obtain insights and enable the protection of downstream WTs from the wake effects of upstream WTs. Related problems can be mitigated by optimizing the layout pattern of WTs in a wind farm, while also reducing the total cost of wind energy [4-6].

At present, although many wind farms are in operation, the demand for larger, more efficient, and more reliable wind farms is increasing. The key problems of modern wind farms must be solved with the least possible delay. Wind loss and the turbulence intensity in wind farms are two aspects related to the placement pattern of WTs [7]. Turbulent flow in a wind farm is characterized by the interaction and superposition of wakes from multiple WTs. The power loss in a WT caused by the wake effect generated by upwind WTs can easily represent 10–20% of the total power [8]. To design an efficient wind-farm layout for offshore wind farms, it is very important to understand the increase in turbulence and the power loss induced by the WT wakes [9]. Several studies of offshore wind have suggested that wake interactions may persist at distances of up to 5–10D (where D represents the rotor diameter of the WT) downstream of WTs [10]. The wake effect in a wind farm is related to the local wind conditions, WT characteristics, wind-farm layout patterns, and some seasonal factors. There is thus a pressing need to study wake effects,

\* Corresponding author. Tel.: 2766 5863  
E-mail address: hong-xing.yang@polyu.edu.hk

but due to the complexity of the problem, it cannot be fully investigated using only theoretical approaches.

To make better use of wind energy, data from full-scale wake experiments are necessary to guide the wind-energy community. With measured data, the characteristics of wind deficit and turbulence can be studied in depth. Via model development and validation processes, state-of-the-art wind farm models are needed that are based on more comprehensive and accurate wake measurements [11-13]. Wake characterizations based on wind field data can be applied to validate and improve numerical wake models. Such characterizations would also enable the power generated by a wind farm to be more accurately estimated and improved [14]. Advanced experimental wind-field tests of wake steering would also facilitate the study of whether the advantages predicted and observed in simulations can be realized in the field. Wind-field experiments can avoid the typical limitations of wind-tunnel experiments, such as low Reynolds numbers and down-scaled geometric dimensions [15]. Therefore, the interaction between the wakes of multiple WTs must be obtained from full-scale experiments with large wind farms, as have been conducted by the authors of [16-22].

To the best of our knowledge, no reviews of wind-field experiments have been reported to date. This study attempts to fill this research gap. One focus of this study was to comprehensively review full-scale wind-field measurements of the wake effect, including experiments conducted at onshore wind farms, offshore wind farms, and isolated WTs. A second focus was to establish a reference database for various experimental sites, techniques, procedures, difficulties, economic controls, and main results to enhance readers' understanding of full-scale wind-field measurements. In section 2, the measurements obtained at six onshore wind farms are discussed. In section 3, the measurements obtained at five offshore wind farm are presented. In section 4, eight other wind-field measurements are analyzed. In section 5, a measurement of the wake interaction effect is presented, and its main results and the experience gained from performing these measurements are summarized. Lastly, in section 6, the main conclusions of this review are drawn.

## 2. Onshore wind-farm measurements

In this section, the measurements obtained at six typical onshore wind-farms are analyzed, comprising measurements from Goodnoe Hills wind farm (Washington, USA), Sexbierum wind farm (Waadhoeke, The Netherlands), Nørrekær Enge wind farm (Jutland, Denmark), the Energy Research Centre of the Netherlands (ECN) test farm (Wieringermeer, The Netherlands), an central Iowan wind farm (USA), and Myres Hill wind farm (Eaglesham, Scotland, UK).

### 2.1 Measurements

#### 2.1.1 Measurements at Goodnoe Hills wind farm

Three 2.5-MW WTs are erected at Goodnoe Hills, a location close to Goldendale, Washington [23], where the terrain slopes upwards smoothly from west to east, and there is a steep gully in the northwest [24]. Figure 1 shows the layout of the WTs at Goodnoe Hills.

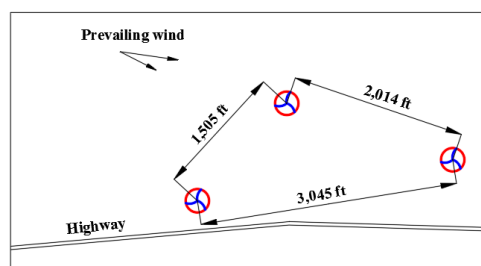


Figure 1. Site layout and distances between wind turbines (red and blue symbols) at Goodnoe Hills, Washington, USA [24].

In 1982, an experimental wind-field project was conducted at the hub height (200 feet) of these WTs [24], in which the wind velocity was captured by a radiosonde suspended from a tethered balloon. A total of 21 hours of data were collected simultaneously from the free stream and the balloon. Measurements were performed to determine the downstream-wind-speed deficit rates at the centerline and the WT drag coefficients. At wind speeds from 30 mph to 45 mph, the deficits in the wind speed reached

approximately 50% at a downwind distance of 3D, and 5% at 5D.

An obvious terrain-induced influence on the flow at the tower site was identified. However, some results that were initially considered to indicate wind deficits were later determined to indicate wind-speed increases, and thus the reason for the deficit could not be determined due to this low experimental accuracy. The non-uniformities of the wind farm, due to terrain irregularities, accounted for some of the observed data scattering. The topography of the wind site was complex, and consequently the wake effect could be either masked or exaggerated.

### 2.1.2 Measurements at Sexbierum wind farm

The experiments at Sexbierum wind farm provided a useful database for validating wake models and WT load-calculation programs. This Dutch wind farm, which is located in Waadhoeke, approximately 4 km from the seashore [25], is situated on flat homogenous terrain with grassland, and has 18 WTs with a rated power level of 300 kW [26], a D of 30.1 m, and a hub height of 35 m. The layout of the Sexbierum wind farm is shown in Figure 2. Surrounding the wind farm, there are seven meteorological masts (M1–M7).

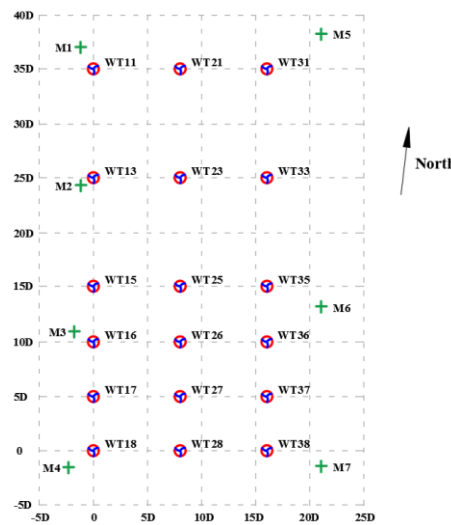


Figure 2. Layout of Sexbierum wind farm in Waadhoeke, The Netherlands [25] (where WT = wind turbine, D = WT rotor diameter).

During 1992, several experiments were conducted at Sexbierum wind farm to collect data on wind velocity, turbulence intensity, and shear stress at WT downwind distances of 2.5D, 5.5D, and 8D [25]. WT36 was fitted with instrumentation to study influence of the wake effect on WT load. The wind speed at hub height matched the Weibull frequency distribution, with a scale factor  $a_{hub} = 8.6 \text{ m/s}$  and a shape factor  $k_{hub} = 2.1$ . The average wind speed was 7.6 m/s.

The monitored quantities comprised the fast-rate wind speed in wakes, WT power, and fatigue load. At  $x = 2.5D$ , the wake profile deviated significantly from a Gaussian shape, with this deviation disappearing at greater distances. At the same position, the turbulence intensity peaked at the maximum wind speed gradient and then disappeared after  $x = 5.5D$ . The courses of the individual shear stresses were qualitatively explained based on the assumption that the wind velocity experienced a gradient change in the wake. These data also enabled a comparison of the power output of different wind directions [26].

### 2.1.3 Measurements at Nørrekær Enge wind farm

The Nørrekær Enge II wind farm is situated at the southern bank of the Limfjord in the northern area of Jutland, Denmark. The terrain of the wind farm is generally very flat, but there are slight irregularities, the largest of which is a 50-m hill in the south. The wind farm has 42 stall-regulated WTs with a rated power of 300 kW. The WTs are fixed in two regular  $7 \times 3$  grids. Figure 3 shows the layout of the Nørrekær Enge II wind farm.

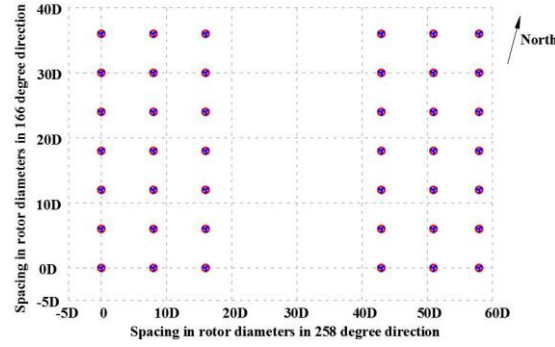


Figure 3. Layout of Nørrekær Enge II wind farm in Jutland, Denmark [26] (where D = wind-turbine rotor diameter).

This wind farm was used to demonstrate the effectiveness of Garrad Hassan WindFarmer (GH Wind Farmer) software for predicting the power output with a wake effect [26]. The data included the power output from all of the WTs, which were averaged over a number of 10-min periods, with the wind blowing along the lines of the WTs.

For a wind direction of  $166^\circ$ , the mean wind speed and power data were grouped by wind speed. Thirteen data points were applied to determine the average power output of each WT. The mean wind speed was approximately 8 m/s at all of the points. The standard deviations (SDs) of these means were also the same. For a wind direction of  $258^\circ$ , the powers of the front-row WTs in the wind farm were used to calculate the mean ambient wind-speed. There was generally good agreement between the predictions made by GH WindFarmer and the measured results. For a wind direction of  $166^\circ$ , the software tended to overestimate the power of the third and fourth WT rows. For a wind direction of  $258^\circ$ , the power of the third line was over-predicted.

#### 2.1.4 Measurements at ECN test farm

The ECN Wind Turbine Test Station Wieringermeer is situated on flat farmland [27] 35 km northeast of the ECN premises in the Netherlands [28]. The test wind farm is equipped with a 108-m meteorological measurement mast and five rows of 2.5-MW WTs, each with a hub height of 80 m. The WTs are installed in a line with a uniform spacing of  $3.8D$  [29]. Figure 4 shows the dimensions and direction of the wind farm.

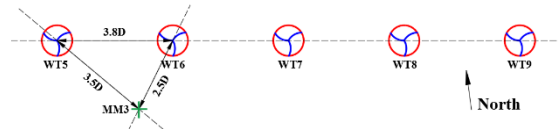


Figure 4. Dimensions and direction of ECN test farm in Wieringermeer, The Netherlands [28] (where WT = wind turbine, D = WT rotor diameter, MM3 = measurement mast 3).

To validate models for simulating wakes and designing wind farms, 2-year data were used. The data were collected at the research site in two ways, i.e., by the ECN measurement network with local data acquisition units (Dante systems) and by the central Supervisory, Control, and Data Acquisition (SCADA) system. Most (80%) of the severe power loss was found to be caused by low turbulence with an intensity range of 2–4%. The maximum wind deficits were approximately 45% at a downstream distance of  $2.5D$  and 35% at  $3.5D$ . A wake rotation effect was visible in the vertical velocities up to a downwind distance of  $3.5D$ . The profiles of wind velocity at downstream distances of  $2.5D$  and  $3.5D$  were compared with the preliminary numerical results of ECN's Wakefarm model, which revealed that the width of the wake and the magnitude of the wind deficit were well predicted, but the turbulence behind the rotor was not. The second array of WTs experienced the maximum power loss, which equated to 67% in westerly winds and 73% in easterly winds. An obvious diurnal cycle was reflected in the vertical turbulence intensity, wind shear, and temperature gradient data. In the evening, a positive vertical temperature gradient was observed at a higher wind shear and a much lower turbulence intensity.

### 2.1.5 Measurements at an Iowan wind farm

The Crop Wind Energy Experiments (CWEXs) were conducted at a wind farm in central Iowa [30], where the land is generally flat, with a slope of less than  $0.5^\circ$  from southwest to northeast. Crops were being raised on the wind farm property, primarily soybeans and corn.

#### (1) CWEX-10 and CWEX-11 experiments

The 2-week CWEX-10 was conducted in the summer of 2010, and the 10-week CWEX-11 was conducted the following summer. Figure 5 shows the layout of the test area.

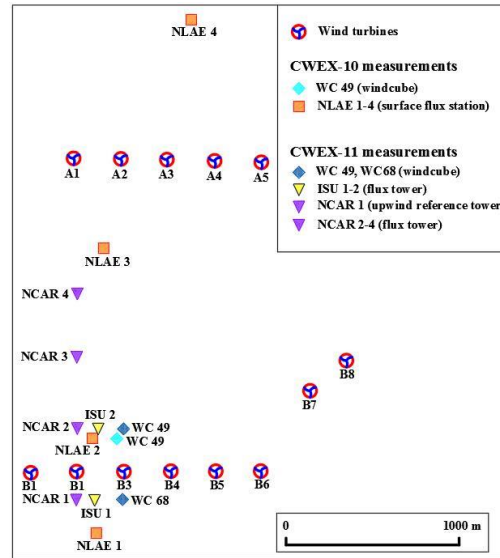


Figure 5. Expanded view of CWEX-10 and CWEX-11 measurement locations in a windfarm in central Iowa, USA [30] (where WC = Windcube, NLAE = National Laboratory for Agriculture and the Environment, ISU = Iowa State University, NCAR = National Center for Atmospheric Research).

Experiments were conducted within and above a corn canopy. In late June, the height of the crop was approximately 1.5 m, and in the middle two weeks of July, the maximum height increased to 2.8 m. Correspondingly, in neutral stratification conditions, the roughness length increased from 0.05 m to 0.4 m.

The results of CWEX-10 and CWEX-11 revealed the influence of one-row WTs on the local environment [30, 31]. CWEX-10 studied the difference between mean variables and surface fluxes in the area surrounding the WTs. In CWEX-11, more flux towers were deployed closer to the WTs. These two experiments identified changes in the flow structure. WTs were found to modify fluxes relevant to the crops, such as  $\text{CO}_2$  and heat. They were also found to enhance the daytime  $\text{CO}_2$  flux down into the crop, but to increase the temperature at night and enhance respiration.

Based on the measured data, Rajewski, et al. [30] proposed three mechanisms that affect the surface micrometeorological conditions leeward of WTs. First, the authors reported that the overhead wake did not reach the surface, but changed the intensity of the turbulence, vertical mixing, and wind profile between the overlying boundary layer and the surface. Second, they found that the wake that intersected the surface enabled the turbulence to modify the microclimate of the surface. Third, the static pressure fields around WTs were found to generate perturbations in the surface flow and produce fluxes within a short distance of the WT line.

#### (2) CWEX-13

The CWEX-13 campaign [32] was conducted in 2013. This measurement location experienced frequent nocturnal low-level jets and strong diurnal cycles of atmospheric stability [33]. Several remote sensing instruments were used to quantify the three-dimensional (3-D) wind speed and turbulence through the WTs. Figure 6 shows a schematic diagram of the wind field. The WT data obtained by scanning light detection and ranging (lidar) are indicated by the red ellipse.

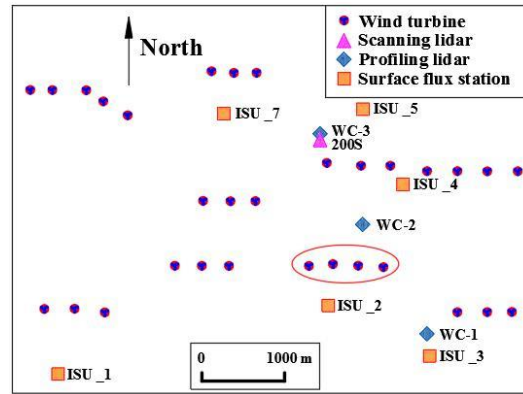


Figure 6. Schematic diagram of the CWEX-13 measurement locations in a windfarm in central Iowa, USA [34] (where WC = Windcube, ISU = Iowa State University).

CWEX-13 focused on the interaction of wakes from multiple WTs under different atmospheric stability conditions, which differed from those discussed in [30, 31, 35] and [36]. The results showed that under unstable conditions, the wake eroded rapidly, indicating that wake measurements should be performed primarily under stable conditions. Under stable conditions, there were significant differences in the wakes of the inner and outer WTs. Wakes at the leading edge of the test area were used to investigate the difference between the outer and inner wakes. The researchers found that strong wind conditions were related to stable conditions, which led to the stretching of the wake distribution. The behavior of wakes from the inner and outer WTs were also found to differ.

With the results of CWEX-13, Bodini, et al. [34] extended the algorithm for single-wake detection proposed by Aitken, et al. [37] to the characterization of multiple wakes. Based on measurements, the algorithm was applied to assess the wind speed deficits, wake boundaries, and wake centerlines. The authors first quantified the influence of ambient wind conditions on the vertical stretching of wakes.

#### 2.1.6 Measurements at Myres Hill wind farm

At the Myres Hill test facility, located outside Eaglesham near Glasgow, Scotland, a long-range inland Galion lidar device is fixed on the southern edge of the wind farm. Position plan indicator (PPI) scan geometries were used to study the wakes of several nearby WTs. Figure 7 shows the location of the Galion device relative to the WTs under study.

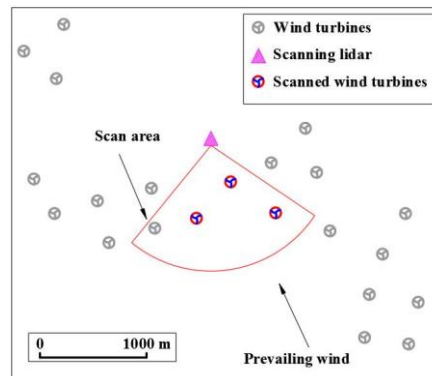


Figure 7. Location of Galion lidar device and wind turbines at the Myres Hill windfarm, Scotland [16].

The wake of the central WT in the surveyed area was modeled using ANSYS WindModeller software, and the direct measurement results were compared with the model results. The horizontal wind speed was estimated by observing the sinusoidal variation in the line-of-sight component with the azimuth. The results obtained from the conventional  $k-\epsilon$  model were the least successful in reproducing the measurements acquired by the Galion lidar device. This lack of agreement in the near wake area occurred because the actuator disc approach was used in the models. Use of the full resolution of the blades was found to improve this situation. Using the  $k-\epsilon$  re-normalization group (RNG) and  $k-\omega$  shear

stress transport (SST) models, good agreement was achieved for the far wake.

## 2.2 Summary of onshore wind-farm measurements

Table 1 summarizes the key information obtained in the onshore wind-farm measurements.

Table 1. Information for onshore wind-farm measurements.

Wind farm	Country	Year of experiment	Duration	Resolution	Wake-measuring device	Terrain
Goodnoe Hills [23] [24]	USA	1982	July 12 to August 1	Maximum sampling rate: 0.5 Hz	Radiosonde suspended from a tethered balloon	Slopes smoothly upward from west to east with a steep gully in the northwest
Sexbierum [25] [26]	The Netherlands	1992	June-November	Sampling rate: 4 Hz	Mobile wind-measuring masts	Flat homogenous terrain with grassland
Nørrekær Enge [26]	Denmark	Before 2003	-	Wind-direction bin: 2.5°	Machine power from all of the WTs	Generally extremely flat, but has some features
ECN test farm [27] [28] [29]	The Netherlands	Since 2003	Several years	Signal frequencies: 1-128 Hz	Dante system and SCADA system	Flat, open farmland
Iowa [30, 31] [32] [33] [34] [30, 31, 35] and [36]	USA	2010-2013	Several weeks	Sonic anemometers: 20 Hz Flux sensors: 1 Hz Wind and turbulence sensor: 0.5 Hz	Lidars	A corn canopy (the height of the canopy varied)
Myres Hill [16]	UK	Before 2011	Several months	-	Galion lidar	Hilly terrain

Some other onshore wind-farm measurements have also provided useful information. More details can be found in the measurements from Samos Island wind park (Greece) [38, 39], AltenbruchII wind farm (Germany) [40], Nygårdsfjellet wind farm (Norway) [41], a Brazilian onshore windfarm [42], and Shiren wind farm (China) [43-46].

Experiments began at onshore wind-farms in 1982 and have continued for more than 38 years. Most of the tested wind farms are located in European countries and the United States. Experiments have typically lasted from months to years. The earliest wake-measurement device was a radiosonde on a tethered balloon, which is now outdated and should no longer be used for reference. More reliable scanning lidars have been widely used by the wind-energy industry to investigate the characteristics of the atmospheric boundary layer. Compared with traditional meteorological measurement towers, these devices are non-intrusive, relatively easy to deploy, and low in maintenance and deployment costs [10, 29]. Data from SCADA systems are also routinely collected for wake analysis. In modern wind-field experiments, the resolution of the wind-speed and wind-direction measurements can fulfil research needs, reaching 0.1 m/s and 1°, respectively. Most of the tested wind farms are located on flat terrain; only a few are located on complex terrain. Ground roughness was considered in CWEX-10 and CWEX-11, and some wake models have been validated against these measured data, but an insufficient range of experiments have been conducted on non-flat terrain, especially on special terrain.

When organizing onshore wind-farm measurements, researchers must consider several factors. The economic cost is closely tied to the complexity of the experiment. If an experiment only requires the collection of some data from instruments installed at the wind farm, the equipment cost may be very low. However, if certain equipment must be purchased or rented for an experiment, these costs may increase and must be carefully considered. Personnel expenditure is also an important factor in any experiment, which is influenced by the nature of the experimental scheme and its duration.

When conducting experiments, the main difficulty is associated with the movement of people and equipment at the wind farm. Therefore, the site conditions have a significant effect on onshore wind-farm experiments. Easier ground conditions, such as terrains with low gradients, make equipment transportation and installation easier and faster, thereby saving the time required for and costs of the entire project. The equipment used in the experiment can greatly affect its overall difficulty. Some small sensors and lidars must be placed on the hub of the WT. Full consideration must be given to the lifting



facilities and personnel safety needed for such tasks

### 3. Offshore wind farm measurements

This section presents analyses of the measurements performed at five offshore wind farms, namely the Vindeby wind farm (2 km from Denmark), Horns Rev wind farm (30 km from Denmark), Middelgrunden wind farm (2 km from Denmark), Alpha Ventus wind farm (75 km from Germany), and Longyuan Rudong Chaojiandai wind farm (4 km from China).

#### 3.1 Measurements

##### 3.1.1 Measurements at Vindeby wind farm

The Vindeby wind farm has eleven 450-kW WTs [47] and is located in Denmark, approximately 2 km from the coast. Two offshore masts (SMW and SMS) and one coastal mast (LM) collect comprehensive meteorological measurements to a height of 48 m. The D of the WTs is 35.5 m and the hub height is 38 m. Figure 8 shows the layout of the wind farm.

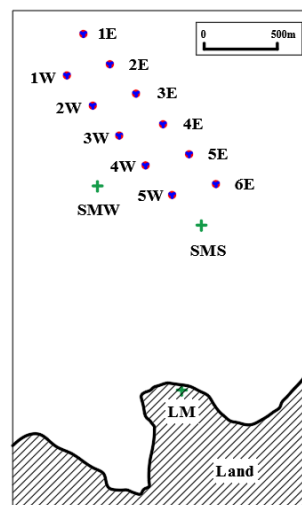


Figure 8. Layout of masts and wind turbines in the Vindeby offshore wind farm, Denmark [47] (where W = western wind turbine, E = eastern wind turbine).

From April 21 to 28, 2001, a total of 36 experiments were conducted. During these experiments, a sonic detection and ranging (sodar) instrument was mounted on the stable Seaworker ship to obtain profiles of the offshore wind speed. The ship was equipped with four anchors and had sufficient room for the sodar on the deck. A series of WT-on, WT-off pairs of experiments were conducted to estimate the wind-speed deficits at the hub height and downstream distances. The measured vertical wind profiles were in good agreement with the mast data. The noise of the WT caused no difficulty in measurements at a height of 100 m. The offshore wind farms within 3 km of the coast could be modeled by onshore wake models.

Barthelmie, et al. [48] evaluated six frequently used wake models, namely the Risø engineering model [49-51], the Risø Wind Atlas Analysis and Applications Program (WAsP) model [52], the Risø analytical model [53], the Farm Layout Program model from University of Oldenburg [54], the ECN Wakefarm model [55], and the computational fluid dynamics (CFD) model from Robert Gordon University [56]. Their evaluation was based on detecting wind speeds in free stream and under wake conditions at downwind distances from  $1.7D$  to  $7.4D$ . A large scaling in the wind deficit was observed at hub height, which had no systematic relationship with the downwind distance. Some models tended to generate higher or lower predictions, but were not fully consistent.

There were measurement uncertainties in the experiments, and some corrections were required in the free stream and wake-measurement stages. The experiment confirmed that sodars could be operated on floating platforms [47]. Based on the cumulative deficit of the momentum, a new method was proposed for predicting the profile of the whole wake. This method was generally correct in its



predictions, and the discrepancies in the measured values were found to be greater than those in the wake model prediction. The prediction spread was relatively even in the single wake cases, although the energy loss during propagation was substantial.

### 3.1.2 Measurements in the Horns Rev 1 wind farm

The Horns Rev 1 offshore wind farm is situated in the North Sea, approximately 30 km west of Esbjerg, Denmark [57]. Three meteorological masts (M2, M6, and M7) are fixed in the area surrounding the wind farm, which comprises 80 WTs in a  $10 \times 8$  matrix. The WTs are numbered as shown in Figure 9.

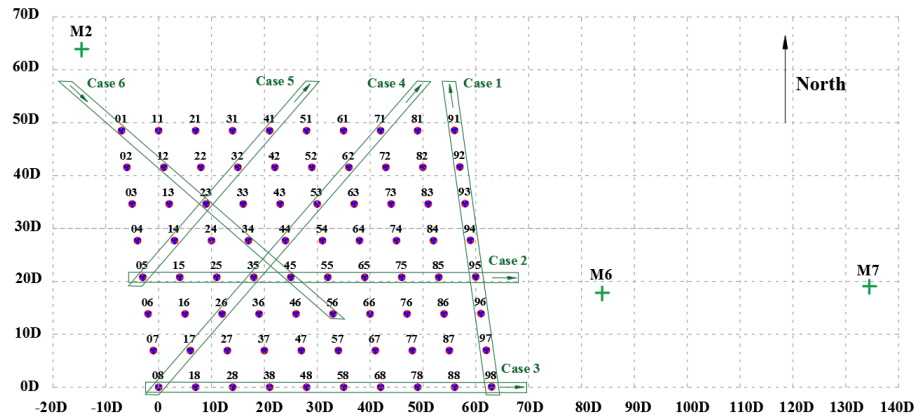


Figure 9. Layout of masts (M) and wind turbines (WTs; blue and red symbols) in the Horns Rev 1 offshore wind farm, Denmark [57] (where D = WT rotor diameter).

#### (1) Study of wake-flow recovery

Jensen, et al. [57] collected operational data using a SCADA system from more than 200 sensors at 10-min intervals, to explore the internal wake effect. Measurements were conducted along three grid-aligned lines and one diagonal line of WTs, as shown in Figure 9 (cases 1–4). The wind speed was analyzed based on four cases, whereas turbulence was analyzed based on cases 2 and 4.

WT35 and WT71 were selected to study the directional dependence of the wake effect. The external wake effect was studied using the data obtained from the three surrounding masts. The results showed a continuous decrease in wind velocity between the first and second WTs in a row, and no significant decrease in wind speed after the second WT. In addition, the results revealed that the influence of wake persisted 6 km downstream of the wind farm. Moreover, the boundary layer remained unstable at pure offshore conditions when the fetch exceeded 15 km.

#### (2) Comparison with wake models

Barthelmie, et al. [8] used measured data from 2005 to compare various models, namely the WAsP linearized model, the Centre of Renewable Energy Sources–Farm model, the GH WindFarmer model, the Wakefarm model from ECN, the model from National Renewable Energy Centre of Spain, and the CFD model from National Technical University of Athens. The wind farm was found to be characterized by a low turbulence intensity of less than 8%, with many operating hours in near-neutral stability. The analysis focused on the westerly flow to maximize the amount of observed data. The three simulation cases were Case 2 (7D spacing), Case 5 (9.4D spacing), and Case 6 (10.4D spacing).

For the narrowest wind direction sector of  $\pm 1^\circ$  and a minimum spacing of 7D, the wind speed at the second row of WTs dropped dramatically, with the powers of the second and subsequent WTs approximately 60% that of the free stream. In wider sectors, the wind reduction at the second WT was less marked, but the wind velocity in the row continued to decrease. The power generation of each WT in a row was normalized to that of the WTs in the free stream. The power generated from the outside rows tended to be less affected by wake losses than that in the central rows.

### 3.1.3 Measurements at Middelgrunden offshore wind farm

The Middelgrunden offshore wind farm is situated in the Øresund Strait, approximately 2 km east of Copenhagen Harbor, Denmark [9]. The wind farm consists of twenty 2-MW WTs with a D of 76 m, a hub height of 64 m, and a WT spacing of  $2.4D$ . Figure 10 shows the layout of the wind farm.

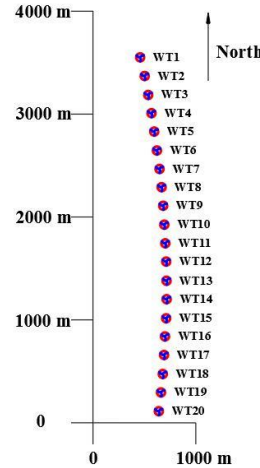


Figure 10. Layout of Middelgrunden offshore wind farm, Denmark [9] (where WT = wind turbine).

The measured data were 10-min averages from 2001 to 2004 obtained using the SCADA system. The variables comprised the mean wind speed, the SD of the wind speed, the yaw angle, the mean power output, and the SD of the power output. The wind speed and wind direction were obtained at heights of 50 m and 48 m, respectively.

When the wind speed was 11 m/s, the turbulence intensity was the smallest (6.5%), and this increased with the wind velocity. Barthelmie, et al. [9] described two methods for estimating turbulence intensity, one based on the mean and SD of wind speed and the other on the mean and SD of the power output. Turbulence intensity estimations derived from power measurements showed better agreement with the data obtained from the meteorological mast.

A comparison of the measurements and wake model results revealed that the model-predicted turbulence intensity was approximately 9% greater than that obtained from the power measurements. Under non-wake conditions, the power-based SD method better represented the ambient turbulence than that based on the nacelle anemometer. When the flow was directly along a row, the turbulence predicted by the WAsP model increased by approximately 20% in absolute terms. The observed wake loss decreased with increasing wind speed. The estimated wind-farm efficiency based on the measured data was 90%, whereas that predicted by the WAsP model was 86%. This discrepancy reveals that the modeling time was independent of the wind-farm power production, and that the actual produced power was 5.7% more than the power estimated by the power curve. In general, the WAsP model data was in good agreement with the measured results.

### 3.1.4 Measurements at Alpha Ventus offshore wind farm

The Alpha Ventus wind farm is located in the North Sea, approximately 75 km from Germany. It consists of twelve 5-MW WTs of two types [58], and the layout of the masts and WTs are shown in Figure 11. The WT Ds are 126 m (AV1–AV6) and 116 m (AV7–AV12), with respective hub heights of 92 m (AV1–AV6) and 91.5 m (AV7–AV12). The offshore met mast FINO1 is located on the west side, 405 m from the nearest WT.

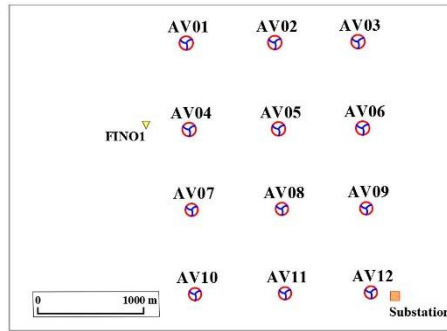


Figure 11. Layout of masts and wind turbines in Alpha Ventus offshore wind farm, Germany [58].

Operational data were evaluated to determine the power reduction experienced by a single WT. By examining the effects of atmospheric stability and turbulence intensity, the wake effects were determined to be more pronounced under stable conditions. For wind speeds of 7–11 m/s, the power deficit under stable conditions was approximately 4% larger than that under unstable conditions. A single wake was found to be wider under stable stratification, which led to a 4% reduction in the power output of the free WT. When the wind speed was higher than the rated speed, the stability no longer had an effect. Generally, consideration of atmospheric stability can improve wake modeling and wind-farm monitoring.

To compare the power reduction at this farm with those of other wind farms, we performed an evaluation to determine whether the power deficits of larger WTs can be scaled up. In comparison with Horns Rev windfarm data, the maximum power deficit of a single WT and a WT along a row of small wind direction sectors at Alpha Ventus windfarm were greater. This might be caused by the different offshore meteorological conditions, which generated greater turbulence intensity at Horns Rev. Therefore, such direct comparisons cannot be made. For present-day wind farms, validation for WTs with larger  $D_s$  is necessary.

### 3.1.5 Measurements at Longyuan Rudong Chaojiandai offshore wind farm

Longyuan Rudong Chaojiandai offshore wind farm, located in 4 km from Jiangsu, China, is a commercial wind farm consisting of multiple types of WTs, and has undergone various stages of construction. Fleming, et al. [59] selected 25 Envision EN136/4-MW WTs at this wind farm to study wake-steering control. These WTs are in the front two rows facing winds coming from the northeast. For this campaign, a single WT was selected as the control.

The experiment was conducted in collaboration with the National Renewable Energy Laboratory and Envision Energy, a smart energy management company and WT manufacturer. To understand the wake dynamics, a yaw control strategy was implemented using the CFD model Simulator for Wind Farm Applications (SOWFA). Another engineering model, the FLOW redirection and induction in steady state (FLORIS), was used for yaw control optimization.

A wake-steering controller was used to increase the amount of power captured, which was similar to the amount predicted by the models. The most easily interpreted results were obtained using the closer spacing (7D), with the 8.5D spacing showing some changes, which were partly due to the limited availability of data. There was also agreement found between the lower expected power loss using the yaw function predicted by SOWFA and the experimentally derived loss. These results have motivated further effort toward the design and development of such controls.

## 3.2 Summary of offshore wind-farm measurements

Table 2 summarizes the key information obtained by the offshore wind farm measurements.

Table 2. Information for offshore wind farm measurements.

Offshore Wind farm	Country	Year of experiment	Duration	Resolution	Wake measurement device
Vindeby [47] [48]	Denmark	2001	April 21 to 28	Wind-speed accuracy: 0.5 m/s Wind-direction accuracy: $\pm 5^\circ$ Height resolution: 5 m	Sodar mounted on a ship

Horns Rev 1 [57] [8]	Denmark	2004-2006	Several years	Wind speed: $\pm 5$ m/s	SCADA system
Middelgrunden [9]	Denmark	2001-2004	Several years	Wind-speed bin: 1 m/s	SCADA system
Alpha Ventus [58]	Germany	2010-2012	Several months	Wind-direction sector: $\pm 2.5^\circ$	Lidar
Longyuan Chaojiandai [59]	Rudong China	2016	First phase: April 3 to August 5 Second phase: August 5 to December 2	Wind-direction bin: $5^\circ$ Data collection rate: 20 Hz	SCADA system

Several offshore wind-farm experiments have been conducted in the past 20 years, mostly at European wind farms. The equipment used in these offshore experiments typically has higher accuracy than other equipment and can withstand the harsh marine environment. Collecting offshore data is much more difficult than collecting onshore data. One main reason for this is that there are few positions available offshore in which to place the measurement devices. Putting these devices on a ship has proven to be a solution, but the accuracy of shipboard devices is strongly influenced by the noise level, inclination, and directional variation of the ship, which must be carefully considered. Lidar has also been a preferred option in recent offshore experiments. Calibrating a lidar device and loading it onto and off of a ship all increase the difficulty of an experiment. Researchers must also complete some of their work on the ship, and the ship movement makes offshore operations more difficult than onshore operations.

Typically, offshore measurements also require greater financial support. The costs of renting a ship and shipping facilities must be included in the research budget and the equipment used for offshore experiments must be capable of withstanding high winds and high-salinity, high-humidity conditions. Rental and insurance expenses increase accordingly. Hiring professional staff to operate the ship increases the overall expenditure. Due to these financial and technical difficulties, offshore experiments using lidars are conducted only for short periods, whereas data collection by the SCADA system of a wind farm can be long-term.

At present, there is little accumulated experience with offshore wind-farm measurements, and there are far less offshore data available than those from onshore installations. Moreover, these offshore data are far from sufficient for wake research. Only offshore wind farms that are very close to the coast can be effectively simulated by onshore wake models. The results from one offshore wind farm cannot be directly applied to another that was WT with different  $D_s$ . Therefore, more experimental work is necessary.

## 4. Isolated WT measurements

Many researchers have performed wake validations for isolated WTs, with the data obtained via remote sensing measurements [2, 13, 17, 37, 60-64]. Some researchers have reconstructed 3-D distributions of WT wakes [15, 65]. In this section, eight measurements related to the isolated WT are analyzed.

### 4.1.1 Lidar measurements of wake dynamics

Between 2004 and 2005, lidar measurement of wake dynamics was performed at the Risø National Laboratory for Sustainable Energy to validate the instrument at the Risø DTU Høvsøre Test Center [2]. This lidar system was installed on the back of the nacelle on a small WT, with a power of 95 kW, a hub height of 29.3 m, and a  $D$  of 19.0 m [13]. The instrument focused on downstream distances from  $1D$  to  $10D$ .

Bingöl, et al. [2] proposed an experimental technique for the direct detection of the instantaneous wind-speed deficit. These measurements validated the hypothesis that due to the mixing caused by small eddies, the wind-speed deficit was passively advected by large eddies and the wake gradually widened. An experiment was conducted to preliminarily verify a wake-meandering model, which essentially used the wake as a passive tracer. Trujillo, et al. [13] developed a method for tracking wake, and tested this based on 2-D lidar measurements. This method delivered the instantaneous transversal wake position, which was quantitatively compared with the predicted model value. The authors hypothesized that a slightly rotating wake would slant downwind to one side and then quickly lose symmetry. This method was applied to two 10-min time-series measurements in stable atmospheric stratification. The measurement and analysis techniques enabled an understanding and recording of full-scale WT wakes.

#### 4.1.2 Wind velocity from multiple wind lidars

Debnath, et al. [66] retrieved vertical wind distributions from three range height indicator (RHI) scans obtained from five simultaneous scanning Doppler wind lidars. The test was conducted at the National Oceanic and Atmospheric Administration's Boulder Atmospheric Observatory in Colorado, USA. The experimental period was from March 2 to May 31, 2015. Three components of wind velocity were retrieved and then compared with the data obtained by profiling wind lidars and sonic anemometers.

The results revealed that the direction and magnitude of the horizontal wind obtained from the triple RHI scans generally had good accuracy. However, the accuracy of the vertical velocity was relatively poor, which may have been due to their small magnitude, the error propagation related to the accuracy of the experimental setup, and the data-retrieval procedure.

#### 4.1.3 Wake Measurements with Coherent Long-Range Pulsed Doppler Wind Lidar

Long-range Doppler lidar measurements for a 5-MW WT were conducted in the northern part of Germany, close to the coastline of Bremerhaven. This WT was the prototype of the Alpha Ventus offshore test site. A 2- $\mu$ m lidar was situated approximately 1820 m northeast of the 5-MW WT (an M5000). Figure 12 shows the layout of the lidar and WTs in the wind farm.

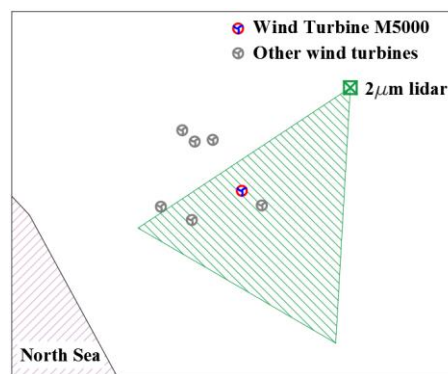


Figure 12. Top view of azimuth scan in a wind farm in Germany [60].

Azimuth and elevation scans were conducted to analyze the distribution of the ambient wind. For the azimuth scanning, the duration was 15 s and the speed was  $2^\circ/\text{s}$ . During elevation scanning, the elevation was continuously increased, but the azimuth angle was fixed. A single elevation-scanning period was 10 s and the scan speed was  $1^\circ/\text{s}$ . Airflow data was measured simultaneously in front of and behind the WT. Käsler, et al. [60] discussed this measurement technique and presented data obtained from the stable nocturnal boundary layer and the diurnal layer. The authors mainly studied the reduction in the wind velocity at a series of downstream distances and proposed a method for capturing the wake. They found the 2- $\mu$ m Doppler lidar to be a reliable tool for studying wind energy and modelling wakes for single WTs and wind parks.

#### 4.1.4 Investigation into the influence of turbulence intensity and wind shear on wake effect

Li, et al. [67] investigated the wind-speed distribution of a WT and the influence of turbulence intensity and wind shear on wake characteristics in the horizontal direction. The tested WT was three-bladed, with a D of 10.0 m, a rated power of 30 kW, and a hub height of 13.4 m. The flow field of the wake zone was determined to be closely related to the operating conditions. To detect the wake distribution, an ultrasonic current meter was installed on the downstream measurement equipment at multiple points.

The WT wake results were analyzed under optimal operating conditions in accordance with the maximum power coefficient [68]. The analysis revealed that the non-dimensional wind speed ratio produced a minimum value near the  $y/R = 0.50$  region, in which  $y$  was the lateral coordinate and  $R$  was blade radius. For both low and high turbulence intensities, the maximum wind-speed deficit was obtained at  $y/R = -0.50$ ,  $z/R = -0.25$ . For all wind-shear indexes, the maximum wind-speed deficit was obtained at  $y/R = -0.50$ ,  $z/R = -0.2$ .

#### 4.1.5 Measurement of a utility-scale WT wake

Hirth, et al. [61] conducted a wake measurement on a single utility-scale WT on October 27, 2011. The data were collected by two 35 GHz Ka-band mobile radars from Texas Tech University. These mobile Ka-band Doppler radar systems were built to obtain data with high spatial and sensitivity resolutions from different aspects of the atmospheric boundary layer.

RHI and PPI scanning techniques were used to analyze various wakes. Preliminary results confirmed that the wind-speed deficit immediately behind the hub was approximately 50%. This result laid the groundwork for using Ka-band radar systems to further analyze wake evolution and distribution, including wake interaction and meandering at large wind farms.

#### 4.1.6 Full-scale wind-field experiment on wake steering

In September 2016, Fleming, et al. [69] began an experimental campaign at the National Wind Technology Center in Boulder, Colorado. There, with the dominant wind direction being from the Rocky Mountains to the west, they operated a utility-scale WT with a yaw misalignment. A lidar was installed on the mount of the WT nacelle.

In the experiment, the yaw controller of the WT was set to track various yaw misalignment set-points, while the lidar was used to scan the wake at several downwind distances. The experiments combined the WT data with incoming wind data collected by a meteorological mast. Then, the measured results were compared with those predicted by FLORIS, a control-oriented wake model used to design wake-steering controllers. The comparisons included the key predictions of FLORIS regarding power loss, wind speed deficit, wake recovery, wake deflection, and wake skew. Agreement was observed between the model results and the observed data. The FLORIS simulations indicated that wake steering may positively affect the annual energy generated by a wind farm.

#### 4.1.7 Wake characterization in complex terrain

The Perdigão experiment was conducted in 2017 in Portugal on a double ridge with a maximum height of 300 m above the local terrain [70]. A team from Cornell University, operating one lidar system at the bottom of the valley, conducted two RHI scans and multiple arc scans every 10 minutes. The Technical University of Denmark team used a dual Doppler lidar system to scan from the northeast ridge. A team from the Deutsches Zentrum für Luft- und Raumfahrt, the German Aerospace Center, used three lidars, two from the predominating wind direction and the third one located on the southwest ridge.

Barthelmie, et al. [71] reported the wake measurements of the three groups, evaluated the advantages of the various scanning strategies, and compared the wake characteristics obtained from different systems. The process used to integrate the datasets was designed to distinguish between common spatial and temporal frameworks. The experiments revealed that the study of wake characterization was more difficult in complex terrain: first, because the flow was complex [72], and second, because the wake behavior itself responded to the flow and the terrain slope [70, 73]. The Perdigão experiment was one of the first to detect wakes by lidar in wind farms with highly complex terrain and to study the advantages of integrating the results of several scanning and lidar systems.

#### 4.1.8 Analytical wake-model validation with nacelle-mounted wind lidars

Another test was conducted at the Kirkwood Community College campus in Iowa. The tested WT was a 2.5-MW Liberty C96 model, which was equipped with a SCADA system that continuously collected data at 10-min intervals. Two pulsed scanning Doppler lidars were installed on the WT nacelle. One was installed upstream to detect incoming wind characteristics, namely turbulence intensity, average wind speed, and vertical and yaw wind-shear. The other lidar was installed downwind to perform horizontal planar scans of the wind-speed deficits.

Carbajo Fuertes, et al. [74] reported the setup, methodology, and results of the single WT's wake characteristics, based on the measurements obtained under various inflow conditions. The authors concluded that a higher inflow turbulence intensity will enhance flow mixing and entrainment in the wake zone, which will then result in faster growth of the wake width, a shorter near-wake length, and faster wind-speed recovery.

## 4.2 Summary of isolated WT measurements

Table 3 shows a summary of key information obtained from isolated WT measurements.

Table 3. Information obtained from isolated WT measurements.

Researchers	Year of experiment	Duration	Resolution	Contribution
Bingöl, et al. [2]; Trujillo, et al. [13]	2004 - 2006	several days	Rectangular grid: 144 and 112 divisions in the horizontal and vertical directions, respectively	Presented an experimental technique for directly detecting the instantaneous wind-speed deficit. Developed and tested a method for tracking a wake based on 2-D lidar measurements.
Debnath, et al. [66]	2015	March 2 to May 31	<i>Sonic anemometers:</i> sampling frequency: 20 Hz <i>Profiling lidar:</i> sampling frequency: 1 Hz <i>scanning lidar:</i> Radial velocity accuracy: 0.5 m/s angular resolution: 0.01°	Determined that data from triple RHI scans accurately capture for horizontal wind velocity but not vertical wind velocity.
Käsler, et al. [60]	2009	several months	Scan speed: 1°/s	Proposed a method for capturing wake data and confirmed the effectiveness of lidar for use in researching of wind energy and model wakes.
Li, et al. [67]	Before 2017	several days	Nacelle orientation: 0±5° Wind velocity change range: 0.5 m/s	Investigated the wind-speed distribution and the influence of turbulence and wind shear on wakes in the horizontal direction.
Hirth, et al. [61]	2011	6 h of effective radar data	Azimuthal (PPI) resolution: 0.352° Elevation (RHI) resolution: 0.1°	Reported that the wind-speed deficit immediately behind the hub was approximately 50%.
Fleming, et al. [69]	2016	several months	Accessible area: a 0.75D × 0.75D square at 1D distance Number of measurement positions: 49 Number of scan distances: 5	Reported that wake steering may positively affect the annual energy generation of a wind farm.
Barthelmie, et al. [71]	2017	May 1 to June 15	Angular resolution: 0.5°/ 1° Physical resolution: 25-60 m	Conducted pioneering wake experiments by lidar in complex terrains and integrated the results obtained from several scanning and lidar systems.
Carbajo Fuertes, et al. [74]	2017	August 20 to October 16	<i>Upstream scanning:</i> Angular resolution: 1–4° Frequency: 1.5-3 Hz <i>Downstream scanning:</i> Angular resolution: 2° Frequency: 2 Hz	Reported that higher turbulence intensity led to a larger wake width, shorter near-wake length, and faster wind recovery.

Some other isolated wind WT measurements have provided useful information. Details can be found in the following papers. Iungo [75] studied the effect of the atmospheric boundary-layer flow on the hub vortex instability on a 2-MW Enercon E-70 WT. Li, et al. [76] used lidars in field experiments to investigate a straight-bladed vertical-axis WT. Wang, et al. [77] collected arc-scan data from a Doppler wind lidar and evaluated the uncertainty associated with the arc-scan geometry. Li, et al. [78] conducted field experiments on the wake behind a 33-kW WT to obtain the velocity distribution. Churchfield, et al. [79] measured wakes and wake deflection due to intentional yaw misalignment under different atmospheric conditions.

To date, many isolated WT measurements have been performed to investigate the wake effect, the use of experimental techniques, and to evaluate equipment. These wake studies have concentrated on single WTs. Lidar has proved to be effective in the study of experimental wakes. Some techniques and models have proved to be useful for experiments and validations, but cannot be widely applied due to the uniqueness of each case.

Compared with wind-field measurements, other factors can be controlled in isolated WT measurements. Experimenters can choose WTs with the appropriate sizes and shapes, or design and build new WTs as needed. The measurement facilities need not be moved to a wind farm, which makes transportation easy and inexpensive. In addition, the experimental time is relatively flexible because isolated WTs can operate at any time and have no constraints from a power grid. Correspondingly, the difficulty and cost of an experiment are closely related to its complexity. Manufacturing a new WT is difficult and time-consuming. When ordering a WT from a manufacturer, its high price must be considered. Generally, isolated WTs are not equipped with many sensors, so experimenters must install all of the necessary equipment and sensors. Although isolated WT measurements often require greater



preparation, the actual experimental duration can be much shorter. Based on historical records, isolated WT experiments typically last several days, with the longest lasting just several months, which is much shorter than the typical multi-year duration of wind-field experiments.

## 5. Measurement of the wake-interaction effect

To date, both onshore and offshore experiments have concentrated on the wake effect of a single WT or wind farm. Few researchers have investigated the wake-interaction effect in detail, especially for WTs under a partial wake effect. In this section, a new experiment is reported to study the wake effect of an upstream WT on a downstream WT. As lidar has proved to be effective in wake measurements, it was applied in this experiment. Some practical experience is also summarized.

### 5.1 Measurements and results

A new experiment has been conducted at the Dongwan Wind Farm, which is affiliated with the Hebei Longyuan Wind Power Co., Ltd. This relatively flat wind farm is located in Baimiaotan Township, Zhangbei County, Zhangjiakou City, China. The wind farm has a total installed capacity of 99 MW, with 52 1.5-MW WTs and 21 1.0-MW WTs. WT3-6 and WT3-7 were the two WTs investigated in this experiment. A lidar was used to measure the wind speed in the downstream space. Table 4 shows the locations of the measured WTs and the lidar sensor.

Table 4 Locations of the measured WTs and lidar sensor.

	Latitude	Longitude
WT3-6	41°12'17"N	114°57'32"E
WT3-7	41°12'09' N	114°57'24"E
Lidar	41°12'25"N	114°57'44"E

Both were 1.0-MW WTs with a D of 54.4 m and a hub height of 70 m. During the experiment, the wind directions were from the north to northeast, so WT3-6 was the upstream WT, and WT3-7 experienced an occasional wake effect. Figure 13 shows some typical data measured at a height of 60 m. In Figure 13(a), WT3-7 is not experiencing a wake effect from WT3-6. In Figure 13(b), WT3-7 is experiencing a partial wake effect from WT3-6. In Figure 13(c), WT3-7 is experiencing a full wake effect from WT3-6. In Figure 13(d), WT3-7 is experiencing wake effects from both WT3-6 and other upstream WTs.

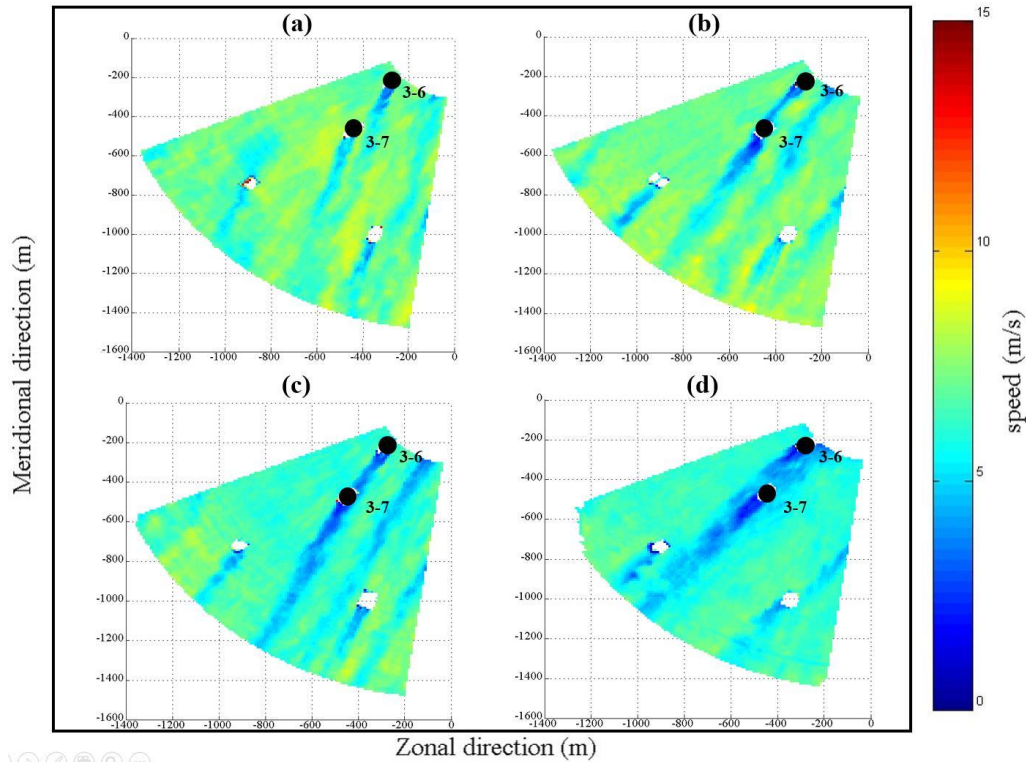


Figure 13. Measured data at a height of 60 m. Time: (a) May 22, 18:47:46; (b) May 22, 19:53:28; (c) May 22, 19:20:41; (d) May 22, 20:37:13.

Based on the measurement results, the wake of the upstream WT not only caused a wind deficit followed by turbulence, but also had an enormous effect on the downstream WT. When WT3-7 was partially affected by the wake of WT3-6, both the length and width of its wake region increased significantly, and the wind-speed deficit was also larger. When WT3-7 was fully affected by the wake of WT3-6, the influence of the wake became more significant. In the extreme situation, when WT3-7 was affected by the wake of several other WTs, the wind-speed deficit was much larger than that in a free stream, and the duration was longer. Interacting wakes thus had a more marked influence on downstream flows than the sum of separate wakes.

## 5.2 Experience obtained from these measurements

These measurements have provided some qualified experience. For wake measurement, mast and sodar/lidar instruments are commonly used. Although meteorological masts are available for long periods, their locations and heights are fixed, so the effective results are very limited. Lidars have become popular for use in recent wake experiments. As these devices weigh dozens of kilograms, when applying lidars in wind farms, comprehensive preparations must be made with respect to the connecting wires, leveling equipment, and installation of effective protective devices. A set of experiments lasting several months may be conducted at a site without the need to move or manipulate the lidar sensors.

The positions of the lidar sensors must also be carefully considered before the collection of data. First, the local prevailing wind directions must be fully considered. Seasonal winds vary greatly in their direction, and WT wakes are sensitive to the wind direction. A small variation in the direction of the angle could cause a large change in the wake. If lidars are placed in downwind positions and the wind direction routinely changes, the wake may sometimes be outside the detection area. In this case, the measured wake length would be too short to study the wake characteristics. Second, the measured downwind distance should not be too large. The commonly used radii of lidars for theoretical investigations may reach several kilometers. But the radii of lidars for actual investigations may be smaller due to certain factors, such as aerosol density and air quality. Air that is either too clean or too dirty will reduce the effective measurement radii. Under strong wind conditions, the wake effect is intense and endures over a long distance. However, as particles are blown away, the aerosol density becomes very low. Therefore, the actual investigation radius should be carefully considered when

planning the position of lidars. Third, ground and aerial obstacles should be avoided. For wind farms in a complex terrain, terrain elevation will affect the choice of lidar position. Most WTs are fixed at high-altitude positions to obtain the maximum wind resources. Given this situation, it is not recommended that lidars be placed in low-altitude positions, because the surrounding inclined ground will limit the scanning space. In addition, obstacles in front of lidars should be avoided, such as high trees and dense arrangements of electrical wires, as these will reduce the scanning space and effective data obtained.

The cost of a wind-field measurement may vary widely depending on the specific time and local issues, with expenses including equipment fees and personnel expenditures. Apart from the meteorological mast installed at the wind farm, some movable and more accurate sensors or devices are needed to collect the required data. For instance, the price of the lidar used for this measurement was approximately one million Chinese yuan (CNY). Two lidars were also rented, for which the total rental expense was CNY50,000 for twenty days. This represents the largest cost of this experiment. The total rental fee comprised the lidar rental, an insurance premium, a one-time installation fee, and a round-trip transportation fee. These expenses are negotiable according to the terms of the lease, whereby a longer rental time can lead to a lower daily rental cost. During the experiment, trained personnel must be present on site to adjust the equipment and monitor the real-time data. Thus, the personnel expenditure is another inevitable and substantial expenditure for the experiment, which comprises transportation fees, living costs, and per diem rates. The duration of wind-field measurements is also affected by the weather conditions. Sometimes, researchers must wait for long periods for specific wind directions or wind speeds, which increases the cost of the experiment. In summary, it is not easy to accurately budget for wind-field measurements, but such budgets must be adequate for a long enough period of time to obtain sufficient data.

Wake steering was not included in this measurement, but it merits mention as it is becoming an active field of research. The overall power production by a wind farm can be improved by coordinating the control of individual WTs co-located within the wind farm. Via effective control strategies, the interactions of the wakes of nearby WTs can be prevented or decreased. When conducting wake-steering experiments at wind farms, some concerns must be addressed in advance. For example, in a commercial wind farm, the primary limitations are often the constraints on data collection. Wind farm data are typically confidential, and developers are often reticent to share original data. If the amount and type of data are restricted, the results may be similarly restricted in their applicability. Another problem is related to the control of the WT yaw angle, as the ability to control the yaw controller may be limited. The control strategy should fully consider the angle limitations and the regulations of using alternate controllers. Furthermore, a significant concern is the additional WT load caused by wake steering. Future studies should focus on the mutual effect on upstream and downstream WTs, and wake-steering loads.

## 6. Conclusion

Research on wind field measurement has been ongoing for more than 38 years. This paper provides a comprehensive overview of historical full-scale wind field measurements of the wind turbine (WT) wake effect and reports a new measurement of the wake-interaction effect. The main conclusions are as follows.

For onshore wind-farm measurements, experiments have been conducted in both flat and complex terrains. The influence of terrain on the WT flow is known to be important, but because of the relatively low experimental accuracy, it is difficult to quantify the resulting wind deficit. Wind velocity and turbulence intensity have been observed at distances 2–3D (where D represents the rotor diameter of the wind turbine) downstream of a WT. This effect diminishes at a distance of 5–7D. The turbulence intensity, vertical temperature gradient, and wind shear have significant diurnal cycles. The wake effect is stronger at night. Some software and wake models have also been validated by onshore wind-farm measurements. Site conditions have had a significant effect on onshore wind-farm experiments. The economic costs associated with personnel and facility expenditures must be carefully considered.

For offshore wind-farm measurements, sodar has proved to be useful for monitoring wind when operated from floating platforms. Several wake models have been studied, but an accurate comparison of the measured values with model results has proved challenging. Some models have tended to predict low or high wakes, but the trends have not been consistent. When estimating turbulence intensity, the power-based standard-deviation method has produced a more practical description of ambient turbulence in the non-wake zone. Turbulence intensity has been determined to be strongly dependent on the wind direction. An enormous reduction in wind speed has been observed between the first two WTs in a row.

The energy output from external WT's has been shown to experience fewer wind losses than that from those in central rows. The observed wake loss has been observed to decrease with increasing wind speed. The collection of offshore data is much more difficult and more expensive than the collection of onshore data. Further model evaluation, better-quality experiments, and more effective measured results are necessary, especially for the case of multiple WT's.

With respect to isolated WT experiments, various measurement methods have been used. In several experiments, the measurement equipment was installed on the mount of a WT's nacelle. Wind lidars have been widely applied to study the characteristic of the atmospheric boundary layer. Doppler lidar has become a well-accepted tool for research in the wind-energy industry and can facilitate the improvement of wake models for single WT's and wind farms. Measurement and analysis techniques have proven to have great potential for understanding and recording full-scale wakes. A nacelle-mounted lidar on a WT with yaw misalignment was used to study the concept of closed-loop wake redirection, based on feedback from lidar sensors regarding actual wake positions. Range height indicator (RHI) and PPI position plan indicator (PPI) scanning techniques have been applied to analyze different wakes. The opportunity to detect wakes with lidar has been demonstrated in a complex-terrain wind farm, as has the capability for studying the advantages of integrating data from several scanning and lidar systems.

A new experiment has been conducted to investigate the influence of an upstream wake on a downstream WT, which fills a research gap on the wake interaction effect. According to the analysis, the wake-interaction effect is so large that it cannot be unconditionally ignored. When a WT is subject to wake effects from several other WT's, the wind-speed deficit is much larger than from a free stream, and the duration is longer. Wake interactions have a more severe influence on downstream flows than the sum of separate wakes. Some field-test experiences were discussed, and related matters that merit attention, such as economic considerations, and advanced wake-steering technology. A consideration of these experiences will contribute to the design of future wind-field experiments.

Although some research has been conducted on the wake effect through wind-field measurements, further efforts are needed, as follows. (1) With respect to onshore wind, measurements in complex terrain are far from sufficient. Experimental data and experience in more complex and typical terrains are needed. (2) The vast majority of previous experiments have been conducted at onshore wind farms. However, with the development of the offshore wind industry, more attention must be given to the experimental study of offshore wind energy. (3) More and better-quality measurements of the effect of multiple WT's are required. There remains an urgent need to further evaluate wake models for multiple WT's. (4) Attention must be paid to the relationship between inflows and wakes, as previous experiments have only measured wakes downstream of a WT, which cannot explain or predict the development of wakes.

## Acknowledgement

The work described in this paper was financially supported by the Research Institute for Sustainable Urban Development (RISUD) with account number of BBW8 and the FCE Dean Research project with account number of ZVHL, The Hong Kong Polytechnic University. The work was also supported by the National Natural Science Foundation of China (No.51606068).

## References

- [1] H. F. Zhou, H. Y. Dou, L. Z. Qin, Y. Chen, Y. Q. Ni, and J. M. Ko, "A review of full-scale structural testing of wind turbine blades," *Renewable and Sustainable Energy Reviews*, vol. 33, pp. 177-187, 2014/05/01/ 2014.
- [2] F. Bingöl, J. Mann, and G. C. Larsen, "Light detection and ranging measurements of wake dynamics part I: one - dimensional scanning," *Wind Energy: An International Journal for Progress and Applications in Wind Power Conversion Technology*, vol. 13, no. 1, pp. 51-61, 2010.
- [3] J. Lundquist, M. Churchfield, S. Lee, and A. Clifton, "Quantifying error of lidar and sodar Doppler beam swinging measurements of wind turbine wakes using computational fluid dynamics," *Atmospheric Measurement Techniques (Online)*, vol. 8, no. NREL/JA-5000-62369, 2015.
- [4] H. Sun, H. Yang, and X. Gao, "Investigation into spacing restriction and layout optimization of wind farm with multiple types of wind turbines," *Energy*, vol. 168, pp. 637-650, 2019/02/01/ 2019.

- [5] H. Sun, X. Gao, and H. Yang, "Investigation into offshore wind farm repowering optimization in Hong Kong," *International Journal of Low-Carbon Technologies*, vol. 14, no. 2, pp. 302-311, 2019.
- [6] H. Sun, H. Yang, and X. Gao, "Study on offshore wind farm layout optimization based on decommissioning strategy," *Energy Procedia*, vol. 143, pp. 566-571, 2017.
- [7] L. P. Chamorro and F. Porte-Agel, "Turbulent flow inside and above a wind farm: a wind-tunnel study," *Energies*, vol. 4, no. 11, pp. 1916-1936, 2011.
- [8] R. J. Barthelmie *et al.*, "Modelling and Measuring Flow and Wind Turbine Wakes in Large Wind Farms Offshore," *Wind Energy*, vol. 12, no. 5, pp. 431-444, Jul 2009.
- [9] R. J. Barthelmie, S. T. Frandsen, M. N. Nielsen, S. C. Pryor, P. E. Rethore, and H. E. Jorgensen, "Modelling and measurements of power losses and turbulence intensity in wind turbine wakes at Middelgrunden offshore wind farm," *Wind Energy*, vol. 10, no. 6, pp. 517-528, Nov-Dec 2007.
- [10] R. J. Barthelmie *et al.*, "Quantifying the Impact of Wind Turbine Wakes on Power Output at Offshore Wind Farms," *Journal of Atmospheric and Oceanic Technology*, vol. 27, no. 8, pp. 1302-1317, Aug 2010.
- [11] H. Sun and H. Yang, "Study on an innovative three-dimensional wind turbine wake model," *Applied Energy*, vol. 226, pp. 483-493, 2018/09/15/ 2018.
- [12] H. Sun and H. Yang, "Numerical investigation of the average wind speed of a single wind turbine and development of a novel three-dimensional multiple wind turbine wake model," *Renewable Energy*, vol. 147, pp. 192-203, 2020/03/01/ 2020.
- [13] J. J. Trujillo, F. Bingöl, G. C. Larsen, J. Mann, and M. Kühn, "Light detection and ranging measurements of wake dynamics. Part II: two - dimensional scanning," *Wind Energy*, vol. 14, no. 1, pp. 61-75, 2011.
- [14] H. Sun and H. Yang, "Study on three wake models' effect on wind energy estimation in Hong Kong," *Energy Procedia*, vol. 145, pp. 271-276, 2018/07/01/ 2018.
- [15] G. V. Iungo, Y.-T. Wu, and F. Porté-Agel, "Field measurements of wind turbine wakes with lidars," *Journal of Atmospheric and Oceanic Technology*, vol. 30, no. 2, pp. 274-287, 2013.
- [16] P. J. Clive, I. Dinwoodie, and F. Quail, "Direct measurement of wind turbine wakes using remote sensing," *Proc. EWEA 2011*, 2011.
- [17] V.-M. Kumer, J. Reuder, B. Svardal, C. Sætre, and P. Eecen, "Characterisation of Single Wind Turbine Wakes with Static and Scanning WINTWEX-W LiDAR Data," *Energy Procedia*, vol. 80, pp. 245-254, 2015/01/01/ 2015.
- [18] B. D. Hirth, J. L. Schroeder, W. S. Gunter, and J. G. Guynes, "Coupling Doppler radar - derived wind maps with operational turbine data to document wind farm complex flows," *Wind Energy*, vol. 18, no. 3, pp. 529-540, 2015.
- [19] B. D. Hirth, J. L. Schroeder, Z. Irons, and K. Walter, "Dual - Doppler measurements of a wind ramp event at an Oklahoma wind plant," *Wind Energy*, vol. 19, no. 5, pp. 953-962, 2016.
- [20] H. Wang and R. Barthelmie, "Wind turbine wake detection with a single Doppler wind lidar," in *Journal of Physics: Conference Series*, 2015, vol. 625, no. 1, p. 012017: IOP Publishing.
- [21] S. Aubrun, E. T. Garcia, M. Boquet, O. Coupiac, and N. Girard, "Wind turbine wake tracking and its correlations with wind turbine monitoring sensors. Preliminary results," in *Journal of Physics: Conference Series*, 2016, vol. 753, no. 3, p. 032003: IOP Publishing.
- [22] F. Zhao *et al.*, "Experimental study on wake interactions and performance of the turbines with different rotor-diameters in adjacent area of large-scale wind farm," *Energy*, vol. 199, p. 117416, 2020/05/15/ 2020.
- [23] T. G. Zambrano and G. W. Gyatt, "WAKE STRUCTURE MEASUREMENTS AT THE MOD-2 CLUSTER TEST FACILITY AT GOODNOE HILLS, WASHINGTON," *IEEE Proceedings A: Physical Science. Measurement and Instrumentation. Management and Education. Reviews*, Article vol. 130, no. 9, pp. 562-565, 1983.
- [24] P. B. S. Lissaman, T. G. Zambrano, and G. W. Gyatt, "Wake structure measurements at the Mod-2 cluster test facility at Goodnoe Hills," *Article* 1983.
- [25] J. Cleijne, "Results of sexbierum wind farm: single wake measurements," 1993.
- [26] W. Schlez, A. Tindal, and D. Quarton, "GH wind farmer validation report," Garrad Hassan and Partners Ltd, Bristol, 2003.
- [27] P. Eecen *et al.*, "Measurements at the ECN wind turbine test location Wieringermeer," in *Proc. EWEA*, 2006.
- [28] L. A. H. MacHielse, P. J. Eecen, H. Kortterink, S. P. Van Der Pijl, and J. G. Schepers, "ECN test farm measurements for validation of wake Models," in *European Wind Energy Conference and Exhibition 2007, EWEA 2007*, 2007, vol. 1, pp. 172-181.

- [29] J. G. Schepers, T. S. Obdam, and J. Prospathopoulos, "Analysis of wake measurements from the ECN Wind Turbine Test Site Wieringermeer, EWTW," *Wind Energy*, vol. 15, no. 4, pp. 575-591, May 2012.
- [30] D. A. Rajewski *et al.*, "Crop wind energy experiment (CWEX): observations of surface-layer, boundary layer, and mesoscale interactions with a wind farm," *Bulletin of the American Meteorological Society*, vol. 94, no. 5, pp. 655-672, 2013.
- [31] M. E. Rhodes and J. K. Lundquist, "The effect of wind-turbine wakes on summertime US midwest atmospheric wind profiles as observed with ground-based doppler lidar," *Boundary-Layer Meteorology*, vol. 149, no. 1, pp. 85-103, 2013.
- [32] J. K. Lundquist *et al.*, "Lidar observations of interacting wind turbine wakes in an onshore wind farm," in *EWEA meeting proceedings*, 2014, pp. 10-13.
- [33] B. J. Vanderwende, J. K. Lundquist, M. E. Rhodes, E. S. Takle, and S. L. Irvin, "Observing and simulating the summertime low-level jet in central Iowa," *Monthly Weather Review*, vol. 143, no. 6, pp. 2319-2336, 2015.
- [34] N. Bodini, D. Zardi, and J. K. Lundquist, "Three-dimensional structure of wind turbine wakes as measured by scanning lidar," *Atmospheric Measurement Techniques*, vol. 10, no. 8, pp. 2881-2896, Aug 2017.
- [35] J. D. Mirocha *et al.*, "Investigating wind turbine impacts on near-wake flow using profiling lidar data and large-eddy simulations with an actuator disk model," *Journal of Renewable and Sustainable Energy*, vol. 7, no. 4, p. 043143, 2015.
- [36] J. C. Lee and J. K. Lundquist, "Observing and Simulating Wind-Turbine Wakes During the Evening Transition," *Boundary-Layer Meteorology*, vol. 164, no. 3, pp. 449-474, 2017.
- [37] M. L. Aitken, R. M. Banta, Y. L. Pichugina, and J. K. Lundquist, "Quantifying wind turbine wake characteristics from scanning remote sensor data," *Journal of Atmospheric and Oceanic Technology*, vol. 31, no. 4, pp. 765-787, 2014.
- [38] C. G. Helmis, K. H. Papadopoulos, D. N. Asimakopoulos, P. G. Papageorgas, and A. T. Soilemes, "An experimental study of the near-wake structure of a wind turbine operating over complex terrain," *Solar Energy*, vol. 54, no. 6, pp. 413-428, 1995/06/01/ 1995.
- [39] J. Whale, K. H. Papadopoulos, C. G. Anderson, C. G. Helmis, and D. J. Skyner, "A study of the near wake structure of a wind turbine comparing measurements from laboratory and full-scale experiments," *Solar Energy*, vol. 56, no. 6, pp. 621-633, Jun 1996.
- [40] B. Subramanian, N. Chokani, and R. S. Abhari, "Experimental analysis of wakes in a utility scale wind farm," *Journal of Wind Engineering and Industrial Aerodynamics*, vol. 138, pp. 61-68, 2015/03/01/ 2015.
- [41] F. Seim, A. R. Gravdahl, and M. S. Adaramola, "Validation of kinematic wind turbine wake models in complex terrain using actual windfarm production data," *Energy*, vol. 123, pp. 742-753, Mar 2017.
- [42] G. S. Bohme, E. A. Fadigas, A. L. V. Gimenes, and C. E. M. Tassinari, "Wake effect measurement in complex terrain - A case study in Brazilian wind farms," *Energy*, vol. 161, pp. 277-283, Oct 2018.
- [43] H. Sun, X. Gao, and H. Yang, "Validations of three-dimensional wake models with the wind field measurements in complex terrain," *Energy*, vol. 189, p. 116213, 2019/12/15/ 2019.
- [44] H. Sun, X. Gao, and H. Yang, "Experimental study on wind speeds in a complex-terrain wind farm and analysis of wake effects," *Applied Energy*, vol. 272, p. 115215, 2020/08/15/ 2020.
- [45] X. Gao *et al.*, "Investigation of wind turbine performance coupling wake and topography effects based on LiDAR measurements and SCADA data," *Applied Energy*, vol. 255, p. 113816, 2019/12/01/ 2019.
- [46] X. Gao *et al.*, "Investigation and validation of 3D wake model for horizontal-axis wind turbines based on filed measurements," *Applied Energy*, vol. 260, p. 114272, 2020/02/15/ 2020.
- [47] R. J. Barthelmie *et al.*, "Offshore wind turbine wakes measured by sodar," *Journal of Atmospheric and Oceanic Technology*, vol. 20, no. 4, pp. 466-477, Apr 2003.
- [48] R. J. Barthelmie *et al.*, "Comparison of wake model simulations with offshore wind turbine wake profiles measured by sodar," *Journal of Atmospheric and Oceanic Technology*, vol. 23, no. 7, pp. 888-901, Jul 2006.
- [49] G. C. Larsen, J. Højstrup, and H. A. Madsen, "Wind fields in wakes," in *1996 European Union wind energy conference. Proceedings*, 1996: HS Stephens & Associates.
- [50] G. C. Larsen, I. Carlen, and G. Schepers, "Fatigue life consumption in wake operation," in *2nd IEA Symposium on Wind Conditions for Wind Turbine Design*, 1999, pp. 77-82: Technical University of Denmark. Department of Fluid Mechanics.

- [51] G. C. Larsen, H. A. Madsen, and N. N. Sørensen, "Mean wake deficit in the near field," in *2003 European Wind Energy Conference and Exhibition*, 2003: European Wind Energy Association (EWEA).
- [52] I. Katic, J. Højstrup, and N. O. Jensen, "A simple model for cluster efficiency," in *European wind energy association conference and exhibition*, 1986, pp. 407-410.
- [53] S. Frandsen *et al.*, "Analytical modelling of wind speed deficit in large offshore wind farms," *Wind energy*, vol. 9, no. 1 - 2, pp. 39-53, 2006.
- [54] J. F. Ainslie, "Calculating the flowfield in the wake of wind turbines," *Journal of Wind Engineering and Industrial Aerodynamics*, vol. 27, no. 1-3, pp. 213-224, 1988.
- [55] A. Crespo, J. Hernandez, E. Fraga, and C. Andreu, "Experimental validation of the UPM computer code to calculate wind turbine wakes and comparison with other models," *Journal of Wind Engineering and Industrial Aerodynamics*, vol. 27, no. 1-3, pp. 77-88, 1988.
- [56] M. Magnusson, K. Rados, and S. Voutsinas, "A study of the flow downstream of a wind turbine using measurements and simulations," *Wind Engineering*, pp. 389-403, 1996.
- [57] L. Jensen, C. Mørch, P. Sørensen, and K. Svendsen, "Wake measurements from the Horns Rev wind farm," in *European wind energy conference*, 2004, vol. 9.
- [58] A. Westerhellweg, B. Cañadillas, F. Kinder, and T. Neumann, "Wake measurements at alpha ventus—dependency on stability and turbulence intensity," in *Journal of Physics: Conference Series*, 2014, vol. 555, no. 1, p. 012106: IOP Publishing.
- [59] P. Fleming *et al.*, "Field test of wake steering at an offshore wind farm," *Wind Energ. Sci.*, vol. 2, no. 1, pp. 229-239, 2017.
- [60] Y. Käsler, S. Rahm, R. Simmet, and M. Kühn, "Wake measurements of a multi-MW wind turbine with coherent long-range pulsed Doppler wind lidar," *Journal of Atmospheric and Oceanic Technology*, vol. 27, no. 9, pp. 1529-1532, 2010.
- [61] B. D. Hirth, J. L. Schroeder, W. S. Gunter, and J. G. Guynes, "Measuring a utility-scale turbine wake using the TTUKa mobile research radars," *Journal of Atmospheric and Oceanic Technology*, vol. 29, no. 6, pp. 765-771, 2012.
- [62] B. D. Hirth and J. L. Schroeder, "Documenting wind speed and power deficits behind a utility-scale wind turbine," *Journal of Applied Meteorology and Climatology*, vol. 52, no. 1, pp. 39-46, 2013.
- [63] M. L. Aitken and J. K. Lundquist, "Utility-scale wind turbine wake characterization using nacelle-based long-range scanning lidar," *Journal of Atmospheric and Oceanic Technology*, vol. 31, no. 7, pp. 1529-1539, 2014.
- [64] D. Bastine, M. Wächter, J. Peinke, D. Trabucchi, and M. Kühn, "Characterizing wake turbulence with staring lidar measurements," in *Journal of Physics: Conference Series*, 2015, vol. 625, no. 1, p. 012006: IOP Publishing.
- [65] R. M. Banta *et al.*, "3D volumetric analysis of wind turbine wake properties in the atmosphere using high-resolution Doppler lidar," *Journal of Atmospheric and Oceanic Technology*, vol. 32, no. 5, pp. 904-914, 2015.
- [66] M. Debnath *et al.*, "Vertical profiles of the 3-D wind velocity retrieved from multiple wind lidars performing triple range-height-indicator scans," *Atmospheric Measurement Techniques*, vol. 10, no. 2, 2018.
- [67] Q. a. Li, T. Maeda, Y. Kamada, and N. Mori, "Investigation of wake characteristics of a Horizontal Axis Wind Turbine in vertical axis direction with field experiments," *Energy*, vol. 141, pp. 262-272, 2017.
- [68] Q. a. Li, T. Maeda, Y. Kamada, and N. Mori, "Investigation of wake effects on a Horizontal Axis Wind Turbine in field experiments (Part I: Horizontal axis direction)," *Energy*, vol. 134, pp. 482-492, 9/1/ 2017.
- [69] P. Fleming *et al.*, "Full-Scale Field Test of Wake Steering," in *Journal of Physics: Conference Series*, 2017, vol. 854.
- [70] N. Vasiljević *et al.*, "Perdigão 2015: methodology for atmospheric multi-Doppler lidar experiments," *Atmospheric Measurement Techniques*, vol. 10, no. 9, pp. 3463-3483, 2017.
- [71] R. J. Barthelmie, S. C. Pryor, N. Wildmann, and R. Menke, "Wind turbine wake characterization in complex terrain via integrated Doppler lidar data from the Perdigao experiment," in *Journal of Physics: Conference Series*, 2018, vol. 1037.
- [72] A. M. Forsting, A. Bechmann, and N. Trolborg, "A numerical study on the flow upstream of a wind turbine in complex terrain," in *Journal of Physics: Conference Series*, 2016, vol. 753, no. 3, p. 032041: IOP Publishing.
- [73] E. S. Politis, J. Prospathopoulos, D. Cabezon, K. S. Hansen, P. Chaviaropoulos, and R. J.



909 Barthelmie, "Modeling wake effects in large wind farms in complex terrain: the problem, the  
910 methods and the issues," *Wind Energy*, vol. 15, no. 1, pp. 161-182, 2012.

911 [74] F. Carbajo Fuertes, C. D. Markfort, and F. Porté-Agel, "Wind Turbine Wake Characterization  
912 with Nacelle-Mounted Wind Lidars for Analytical Wake Model Validation," *Remote Sensing*,  
913 vol. 10, no. ARTICLE, p. 668, 2018.

914 [75] G. V. Iungo, "Experimental characterization of wind turbine wakes: Wind tunnel tests and wind  
915 LiDAR measurements," *Journal of Wind Engineering and Industrial Aerodynamics*, vol. 149,  
916 pp. 35-39, 2// 2016.

917 [76] Q. Li, T. Maeda, Y. Kamada, T. Ogasawara, A. Nakai, and T. Kasuya, "Investigation of power  
918 performance and wake on a straight-bladed vertical axis wind turbine with field experiments,"  
919 *Energy*, Article vol. 141, pp. 1113-1123, 2017.

920 [77] H. Wang, R. J. Barthelmie, A. Clifton, and S. C. Pryor, "Wind Measurements from Arc Scans  
921 with Doppler Wind Lidar," *Journal of Atmospheric and Oceanic Technology*, vol. 32, no. 11, pp.  
922 2024-2040, Nov 2015.

923 [78] D. S. Li, Y. R. Li, R. N. Li, S. J. Liu, Y. Li, and W. R. Hu, "Field experiment and analysis of the  
924 wake behind a horizontal-axis wind turbine," *Scientia Sinica: Physica, Mechanica et*  
925 *Astronomica*, Article vol. 46, no. 12, 2016, Art. no. 124706.

926 [79] M. Churchfield, Q. Wang, A. Scholbrock, T. Herges, T. Mikkelsen, and M. Sjöholm, "Using  
927 High-Fidelity Computational Fluid Dynamics to Help Design a Wind Turbine Wake  
928 Measurement Experiment," in *Journal of Physics: Conference Series*, 2016, vol. 753.

929